

Kinetic oscillations in the catalytic CO oxidation on Pt(100): Periodic perturbations

R. J. Schwankner,^{a)} M. Eiswirth, P. Möller, and K. Wetzl

Institut für Physikalische Chemie, Universität München, 8 München 2, Federal Republic of Germany

G. Ertl

Fritz-Haber-Institut der Max Planck-Gesellschaft, 1 Berlin 33, Federal Republic of Germany

(Received 23 December 1986; accepted 17 March 1987)

Periodic modulations of oxygen pressure or temperature were applied in the catalytic oxidation of CO on a Pt(100) surface under isothermal, low pressure conditions. Transitions from aperiodic autonomous oscillations to regular phase-locked behavior could be observed. Computer simulations using a stochastic cellular automaton model yielded qualitatively similar results. The spatial distribution in both experiment and simulation varies essentially in phase over the whole surface area under the influence of the periodic perturbation, while wave propagation in the autonomous system causes more irregular overall behavior.

I. INTRODUCTION

The occurrence of self-sustained (autonomous) kinetic oscillations during the catalytic oxidation of CO at well-defined Pt(100) single crystal surfaces and under isothermal low-pressure conditions has been investigated in detail during the past years.¹⁻⁹ These oscillations are coupled with adsorbate induced structural transformations of the topmost layer of platinum atoms, whereby the two phases (1×1 and "hex") exhibit different adsorptive and hence catalytic properties. Wave-like propagation of these transformations across the macroscopic surface area was found to be responsible for spatial self-organization. While the conditions (p_{CO} , p_{O_2} , T) under which autonomous oscillations occur can be established quite reproducibly,⁶ their temporal structure is usually irregular.

The influence of periodic variations of the external parameters on the behavior of homogeneous chemical oscillators has already been extensively studied, both in experiment and theory.¹⁰⁻¹³ As an example we mention the occurrence of "chemical resonance" with a damped BZ oscillator.¹⁴ The present paper describes the results of a first exploratory study of such effects with a heterogeneously catalyzed reaction. Experiments were performed in which the operation parameters p_{O_2} and T , respectively, were periodically disturbed without leaving the respective existence region for autonomous oscillations. In parallel, a recently developed stochastic simulation model for the oscillations, based on the cellular automaton technique,⁹ was applied. These computer simulations were found to reproduce the features of the experimental observations qualitatively well.

II. EXPERIMENTAL

The experiments were performed with a standard UHV system as described previously.^{6,8} The cylindrical Pt single crystal (7 mm diam, 1 mm thickness) was spot-welded between two parallel tantalum wires which permitted resistive heating. The temperature of the sample was measured

by a Chromel-Alumel thermocouple spotwelded to its rear and was feedback-regulated.

Gases of the highest commercially available purity (Linde) were used; CO was further purified over oxisorb (Messer Griesheim). A feedback-controlled gas inlet system (Fig. 1) served to keep the total pressure constant to within 0.1% which was continuously monitored by an ionization gauge (Varian).

Since under typical oscillation conditions p_{CO} is about one order of magnitude smaller than p_{O_2} , small amplitude modulation of p_{CO} would be hard to control. Thus only the parameters p_{O_2} and T were periodically varied. Modulation of the temperature causes simultaneous changes of all activated elementary processes (desorption, reaction, diffusion, and surface phase transition) which prevents straightforward interpretation of the system response, while variation of a partial pressure affects primarily the rate of adsorption of the species in question.

p_{O_2} was modulated by feeding an external signal to the control unit (Fig. 1) which was produced by an RC generator with sinusoidal, triangular, and sawtooth output, respectively, or taken from a microcomputer via IEEE bus and a CI-412 interface (MKS). Pressure modulation with frequencies up to about 0.3 s^{-1} could be produced in this way. At even higher frequencies, the amplitude as recorded by the ionization gauge decreased, and there was an increasing phase shift between external pressure and the pressure inside the vacuum system.

T was periodically changed with sinusoidal forcing characteristic by coupling the frequency generator with the temperature controller.¹⁵ Frequency span (up to 0.05 s^{-1} at 3 K amplitude) was limited by the cooling rate of the sample under operation conditions.

Temporal oscillations were monitored through continuous work function ($\Delta\phi$) measurement by a Kelvin probe. The $\Delta\phi$ signal and the modulated parameter (i.e., the read-out of the ionization gauge or of the temperature control unit) were recorded with a dual channel chart recorder permitting easy identification of the kind of entrainment and of the phase shift. The $\Delta\phi$ signal was also digitized using a

^{a)} Present address: Deutsches Museum, 8 München 22, FRG.

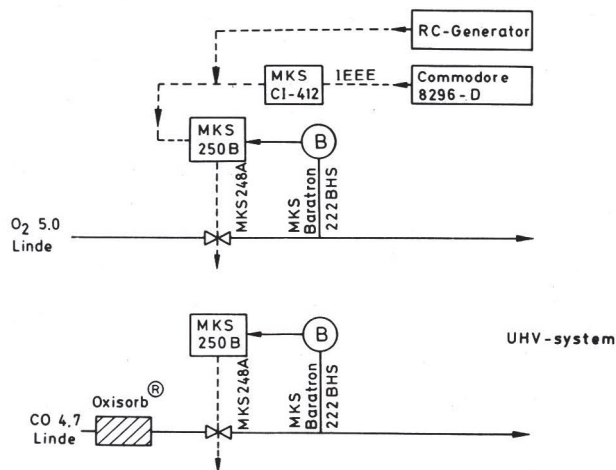


FIG. 1. Schematic diagram of the gas inlet system.

Keithley (196 A) multimeter and read into a microcomputer (Commodore 8296 D). Frequency analysis could thus be achieved by the usual fast Fourier transform technique.¹⁶

LEED investigations at oxygen partial pressures of up to about 10^{-4} Torr became possible by the use of a thoriated Ir filament.^{17,18} Laterally resolved information about the dynamics of surface structural transformation was obtained by the previously described scanning LEED technique.⁸ The spatial resolution is about 1 mm as determined by the diameter of the LEED beam. A two-dimensional scan ("frame") over the whole surface area was recorded within 10 s with a data acquisition rate of 10 s^{-1} . Up to 42 frames could be recorded and stored without interruption, thus providing the opportunity to study several subsequent oscillation cycles.

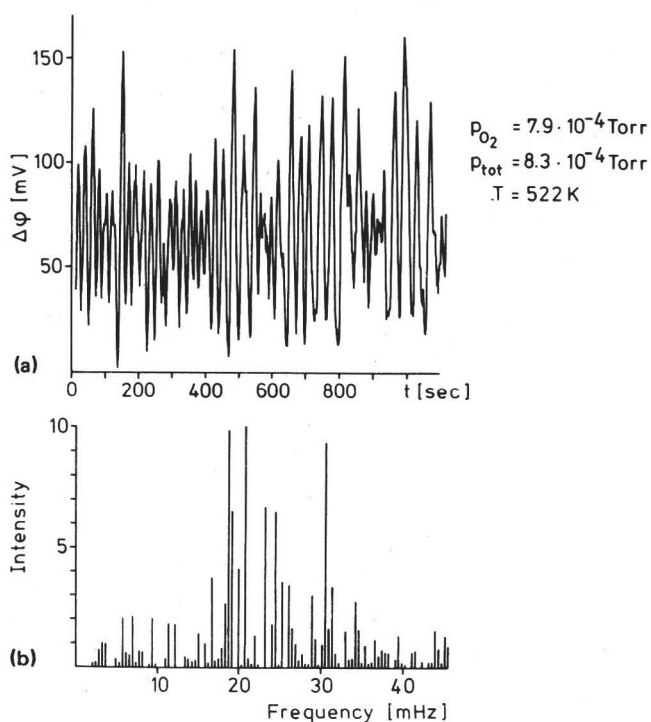
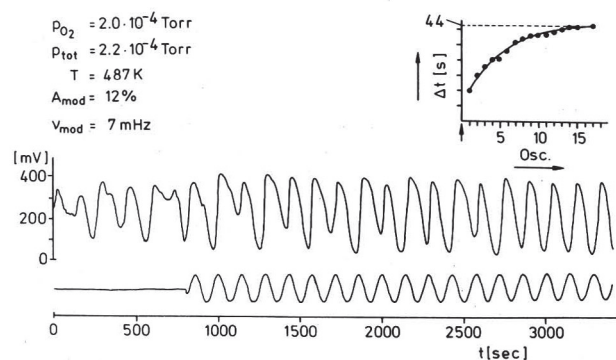


FIG. 2. A typical time series for autonomous oscillations (a) and the corresponding power spectrum (b).

FIG. 3. Transient behavior of the $\Delta\phi$ oscillations after switching on a periodic modulation of the O_2 pressure. The inset shows the time lag Δt between the maxima of $\Delta\phi$ response and p_{O_2} , which reaches a constant value after about 15 periods ("phase locking").

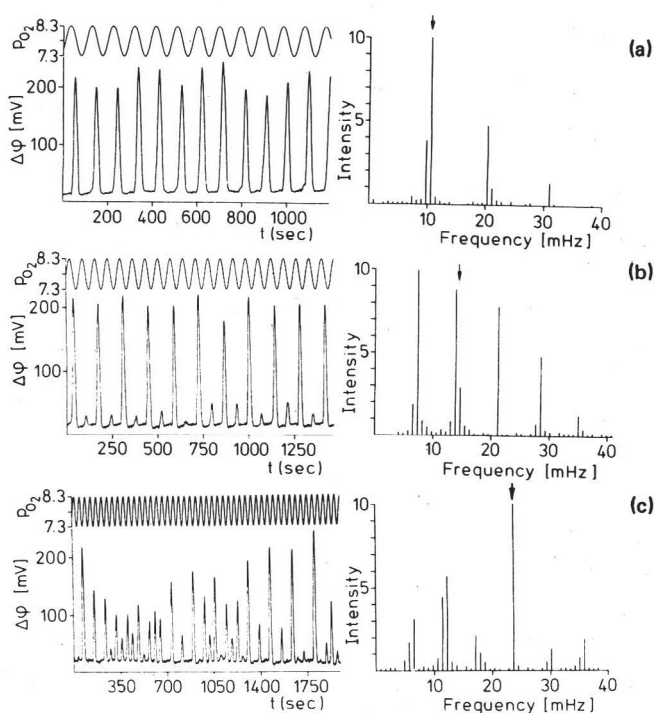
III. RESULTS

A. Work function response

Measurements of the variation of the work function ($\Delta\phi$) with the Kelvin probe reflect the *integral* behavior of the whole surface area ($\sim 35 \text{ mm}^2$). $\Delta\phi$ is essentially governed by the oxygen coverage and parallels the rate of CO_2 formation.⁸

In all measurements the conditions ($p_{\text{CO}}, p_{\text{O}_2}, T$) were first adjusted within the range of autonomous oscillations which were usually aperiodic. A typical example is reproduced in Fig. 2 together with its frequency spectrum.

In a first set of experiments the O_2 pressure was periodically modulated whereby the p_{O_2} amplitude was never so

FIG. 4. Typical time series and corresponding power spectra for three different modulation frequencies as marked by arrows: (a) Harmonic entrainment, $v_r = v_{\text{mod}}$. (b) Alternating big and small oscillations. (c) Irregular response. $p_{\text{O}_2} = 7.8 \times 10^{-4} \text{ Torr}$, $p_{\text{tot}} = 8.3 \times 10^{-4} \text{ Torr}$, $T = 520 \text{ K}$.

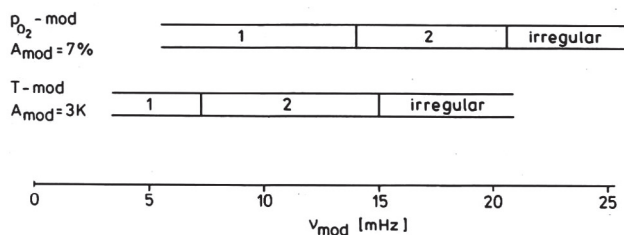


FIG. 5. A plot of the kind of response vs modulation frequency of p_{O_2} (top) and T (bottom). (Conditions as in Fig. 4.)

large as to leave the existence range for autonomous oscillations. As can be seen from Fig. 3, switching on the modulation forces the oscillations to become periodic after an induction period of typically about ten forcing cycles, and the time lag Δt between p_{O_2} and $\Delta\varphi$ maxima becomes constant ("phase-locking") as shown in the inset of this figure. If, on the other hand, the p_{O_2} modulation was switched off, the system returned again within about five cycles to aperiodic behavior. Variation of the modulation frequency ν_{mod} at constant amplitude ($\Delta p_{O_2}/p_{O_2} = 0.07$) caused the system to respond with the same main frequency, $\nu_r = \nu_{mod}$, and with all amplitudes of similar magnitude [harmonic entrainment, Fig. 4(a)], but above a critical perturbing frequency the response consisted of alternating big and small oscillations [period-doubled behavior, Fig. 4(b)], leading to increased Fourier coefficients at $\frac{1}{2}$ and $\frac{3}{2}$ ν_{mod} . At still higher frequencies, the response became irregular without any apparent order in the distribution of amplitudes and with some peaks missing completely [Fig. 4(c)]. There was, however, still a constant phase shift of the maxima. The power spectrum showed additional bands at $\frac{1}{4}$, $\frac{3}{4}$, and $\frac{5}{4}$ ν_{mod} . The frequency bands in which the described types of response occurred are indicated in Fig. 5.

The phase shift δ depends on both the amplitude and the frequency of the perturbation. Figure 6 shows how at fixed ν_{mod} the phase shift increases with modulation amplitude and finally reaches a saturation value. It should be mentioned that in this case for $A_{mod} < 1\%$ the response was aperiodic, between 2% and 4% it consisted of alternating big and small oscillations, and for $A_{mod} > 4\%$, harmonic entrainment took place. If, on the other hand, the amplitude is kept constant, variation of the modulation frequency leads

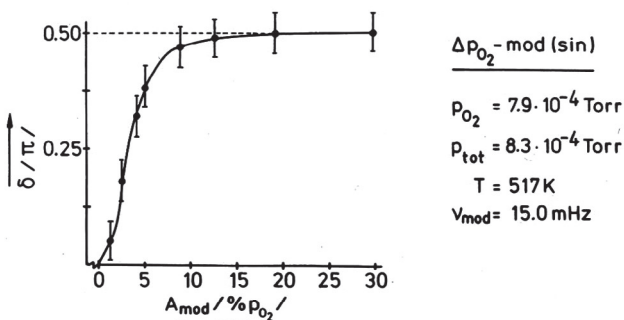


FIG. 6. Phase shift δ vs amplitude of the p_{O_2} modulation at constant frequency.

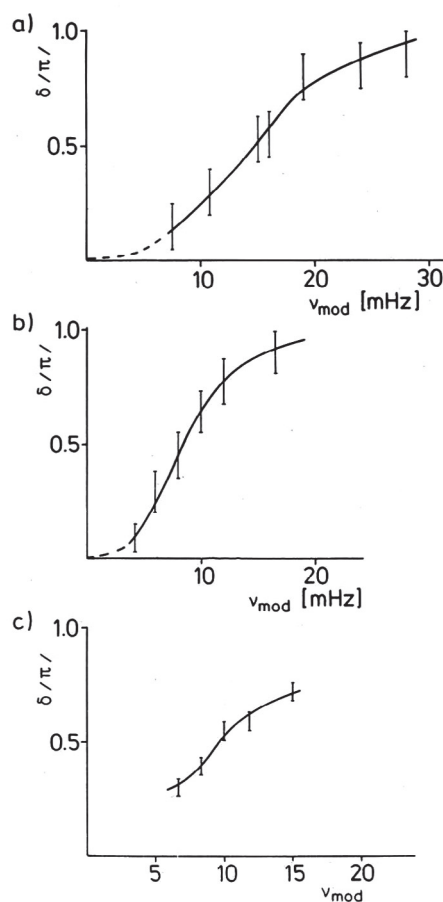


FIG. 7. Phase shift δ as a function of perturbation frequency ν_{mod} at constant amplitudes: (a) Experiment: Modulation of O_2 pressure with conditions as indicated in Fig. 4. (b) Experiment: Modulation of temperature with conditions as indicated in Fig. 4. (c) Computer simulations. Arbitrary frequency ν_{mod} .

to a continuous change of δ as reproduced in Fig. 7(a) from 0 to nearly π . This behavior is reminiscent of a classical resonance effect. It should, however, be reminded that our system exhibits autonomous sustained oscillations in the absence of an external periodic perturbation instead of transient damped oscillations as characteristic of a genuine resonance effect. As a consequence, the amplitude response of the present system shows hardly any indication of a resonance effect, albeit the mean amplitude decreases substantially at higher modulation frequencies. It should be noted, on the other hand, that the system switches to period-doubled behavior around $\delta = \pi/2$.

The autonomous oscillations frequently consist of a fairly rapid increase of $\Delta\varphi$ followed by a slower decay which can be associated with the mechanism of the oscillations^{7,8}: Adsorbed CO is autocatalytically removed from the surface and intermediately replaced by O_{ad} (steep $\Delta\varphi$ rise), and in subsequent slower steps the transformation of the surface structure and buildup of the CO coverage takes place ($\Delta\varphi$ drops). This general tendency is also reflected in a series of measurements in which the temporal shape of the periodic pressure perturbation was altered (Fig. 8). As can be seen from Fig. 8(a), a sinusoidal p_{O_2} modulation caused the oscillations to become rather symmetric, but they still tend to increase

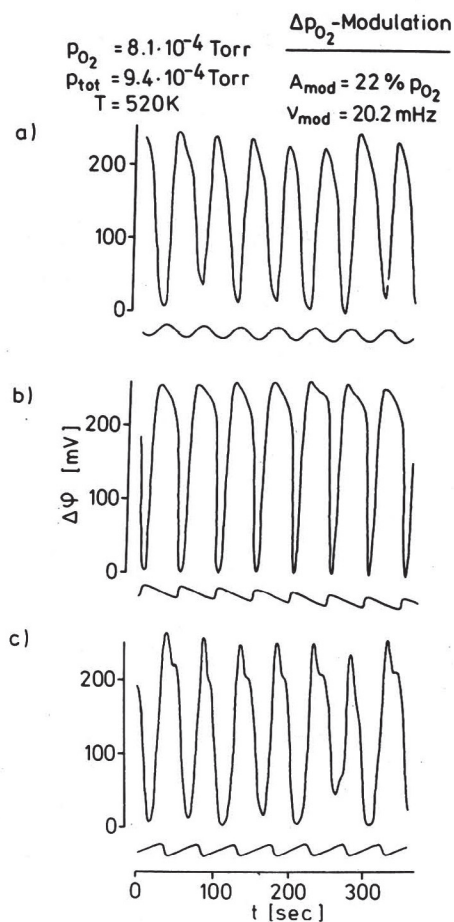


FIG. 8. Influence of the shape of the periodic perturbation on the temporal response of the system.

more steeply than to decay. With a sawtooth modulation of the type indicated in Fig. 8(b) (keeping frequency and modulation constant) the response became more asymmetric in the outlined sense. If, however, the shape of the sawtooth is reversed (i.e., slow increase and rapid decrease) as in Fig. 8(c), the response exhibits a typical shoulder in the decreasing branch, but the $\Delta\phi$ increase is still steep. These results are only intended to demonstrate that even the curve shape of the external modulation is affecting the response of the system, but will not be discussed further.

Periodic variation of temperature instead of oxygen partial pressure led to qualitatively the same phenomena. However, when varying the perturbing frequency with a constant amplitude of 3 K, the transitions to period-doubled and irregular behavior and the increase of phase shift occurred at lower ν_{mod} than when modulating oxygen pressure (Figs. 5 and 7). This is attributed to the fact that a 3 K change in temperature causes a bigger change in (at least) one elementary step than a 7% change in p_{O_2} , thus exhibiting a higher perturbing amplitude.

B. LEED investigations

The temporal oscillations had been found to be associated with a periodic transformation of the surface structure from the hex to the $c2 \times 2-1 \times 1$ phase and back² which can

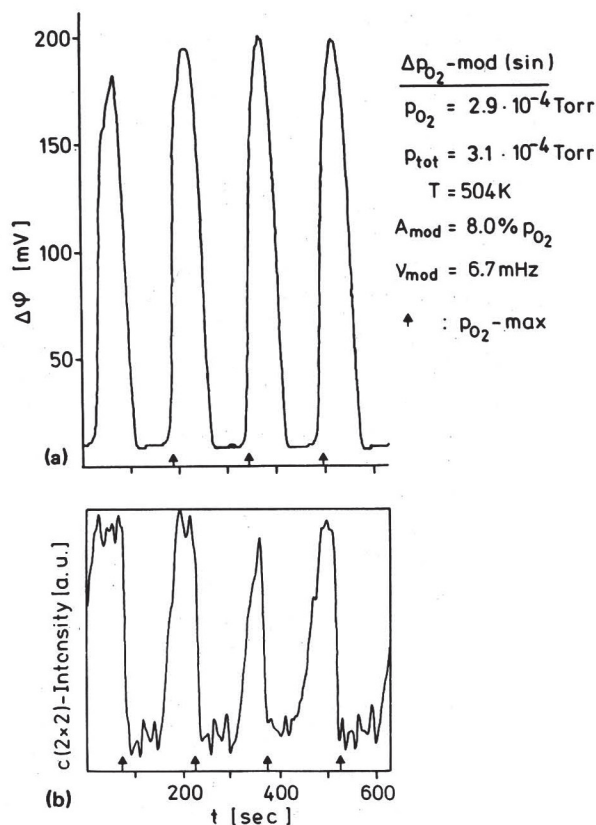


FIG. 9. (a) $\Delta\phi$ time series under the influence of periodic p_{O_2} modulation. The arrows mark the maximum values of p_{O_2} . (b) Corresponding variation of the intensity of a half-order LEED spot.

be studied by LEED. The LEED beam probes about 0.5 mm^2 of the surface area and the scanning technique^{5,8} yields temporally as well as spatially resolved information. In the present study only the $c2 \times 2-1 \times 1$ phase was monitored through analysing the intensity of one of the half-order beams in the LEED pattern which reflects the density of adsorbed CO molecules.

After establishing forced oscillations the sample was turned from the Kelvin probe to the LEED optics and afterwards back again (in order to check reproducibility). Typical $\Delta\phi$ and LEED intensity time series recorded in this way are reproduced in Fig. 9. The arrows denote the intervals at which p_{O_2} reaches its periodic maximum values. These marks coincide with the $\Delta\phi$ increase ($\hat{=}$ increase of oxygen coverage) and with the decrease of the LEED intensity ($\hat{=}$ removal of CO_{ad}). This is in full agreement with the mechanism underlying these processes. It is, however, not trivial that the behavior averaged over the whole surface area (probed by $\Delta\phi$) is in phase with the local properties recorded by LEED—but this will become evident from the spatially resolved LEED data.

Scanning LEED results showing the laterally resolved distribution of the $c2 \times 2-1 \times 1$ intensity ($= \text{CO}_{\text{ad}}$ concentration) taken every 10 s as "snapshots" are reproduced in Figs. 10 and 11. Figure 10 reflects a typical situation found with autonomous oscillations. Here spatial inhomogeneities (reaction zones) start in irregular time intervals and usually at the edges of the sample (but not always at the same place)

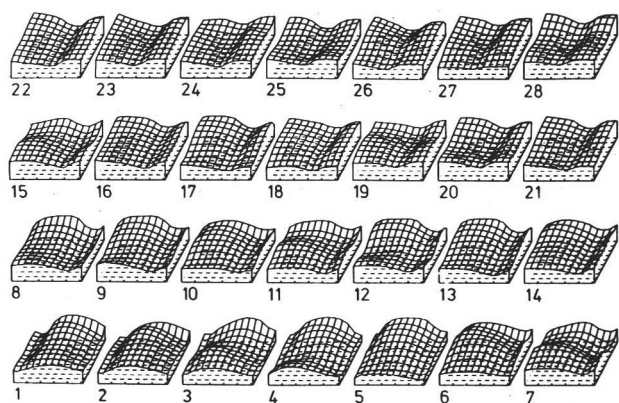


FIG. 10. Scanning LEED data showing the spatial distribution of the half-order spot intensity (reflecting the local CO coverage) during autonomous oscillations. $p_{O_2} = 2.9 \times 10^{-4}$ Torr, $p_{CO} = 2 \times 10^{-5}$ Torr, $T = 514$ K. Each frame is recorded within 10.4 s.

and then propagate wavelike across the whole surface area. These data are qualitatively quite similar to those published previously.^{5,8}

The situation becomes different under conditions of harmonic entrainment (Fig. 11). It turns out that whenever the O_2 pressure reaches its maximum a wave of CO_{ad} removal (= O_{ad} uptake) starts in the region of the upper left corner. These are the frames marked by a triangle in Fig. 11. One frame (10 s) later the CO coverage has been reduced substantially over the whole surface area which recovers slowly and rather homogeneously over the subsequent 40–50 s. In general, under the conditions of forced oscillations the whole surface area becomes more homogeneous and all parts of the surface tend to change their structure more or less simultaneously as synchronized by the external perturbation. As a consequence the spatially integrated behavior as probed by $\Delta\varphi$ becomes more regular.

C. Computer simulations

Based on information about the elementary steps underlying the kinetic oscillations,^{5–8} recently a stochastic model using the cellular automaton technique was developed and successfully applied to simulate autonomous temporal oscil-

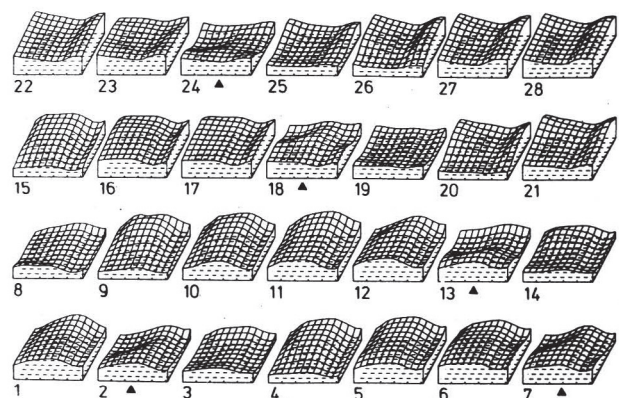


FIG. 11. Scanning LEED data during modulation of the O_2 pressure at $\nu_{mod} = 18.2$ mHz with 8% amplitude. Other parameters as for Fig. 10.

TABLE I. Parameters used in computer simulations (for further explanation see Ref. 9).

O_2 adsorption	0.8
CO adsorption	0.1
Phase transition 1×1 hex	0.07
CO desorption 1×1	0.004 ± 0.001 (25%)
CO desorption hex	0.04 ± 0.01 (25%)

lations and spatial pattern formation.⁹ In this model a two-dimensional lattice of 1560 (20×78) points was used, where each lattice point could exist in one of five different states, namely empty hex or 1×1 , CO-covered hex or 1×1 , and O-covered 1×1 . These states can mutually transform into each other by adsorption of CO or O_2 , desorption of CO, surface reaction (i.e., CO_2 formation), and surface structural transformation. Each of these steps has a finite probability to take place during one cycle in which each of the lattice points was interrogated in a random number sequence. The resulting dynamical behavior is, of course, strongly dependent on the choice of the input parameters.

In order to simulate qualitatively the experimental conditions, a sinusoidal variation of the CO desorption probability was introduced. This is the elementary step exhibiting the largest activation energy and hence temperature dependency: Around 500 K, a temperature variation by 3 K (10) K causes this quantity to change by 25% (60%). (Percentages given as deviations of maximum and minimum from average value.) No *a priori* spatial inhomogeneities (such as trigger compartments) were assumed, similar to some of the examples presented in Ref. 9. The input parameters are listed in Table I and (without modulation) lead to autonomous irregular behavior of the kind shown in Fig. 14 of Ref. 9.

Two typical examples of how a 25% periodic variation of the CO desorption probability affects the temporal response are reproduced together with the associated power spectra in Figs. 12 and 13. Increasing the modulation fre-

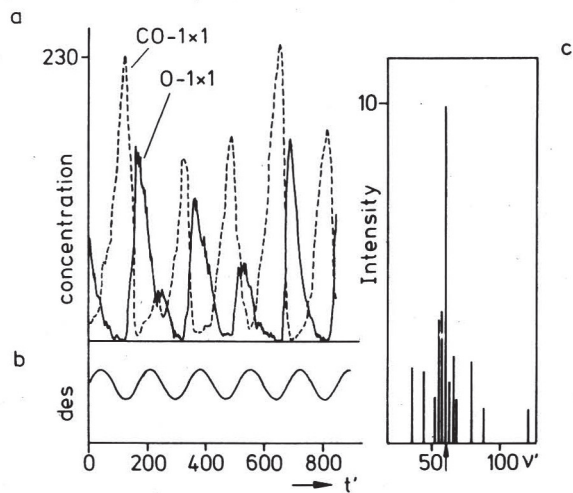


FIG. 12. Computer simulation with periodic modulation of the CO desorption probability (b) leading to harmonic entrainment as can be seen from the power spectrum (c). (a) Temporal variation of $CO-1 \times 1$ and $O-1 \times 1$. The modulation frequency, $\nu'_{mod} = 59$ a.u. is marked by an arrow in (c).

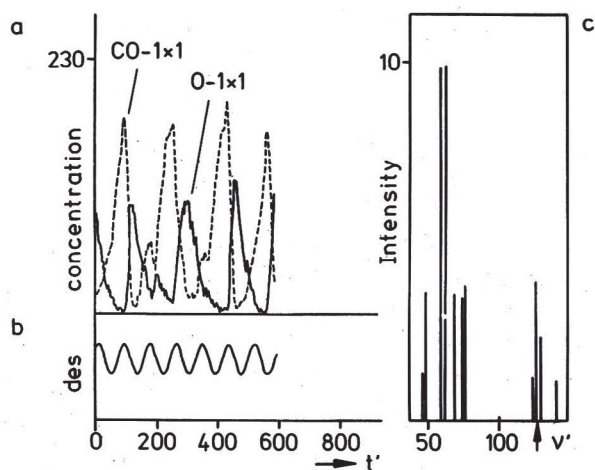


FIG. 13. Similar data as in Fig. 13, except that the modulation frequency $\nu'_{\text{mod}} = 118$ a.u. now is twice the main frequency of the time series.

quency ν'_{mod} caused the computer model to respond with main frequencies $\nu'_1 = \nu'_{\text{mod}}$ and then $\nu'_2 = \frac{1}{2}\nu'_{\text{mod}}$, similar to the experimental situation.

Towards higher modulation frequencies it often turned out that each CO desorption maximum initiated a propagating O_{ad} wave, but every second wave died soon because the time interval was too short to reestablish a high enough CO coverage. This effect shows up in the temporal behavior of

the CO coverage integrated over the whole surface area as a peak with large amplitude followed by a small one or just as a shoulder. It becomes clearly evident from inspection of the time evolution of the spatial pattern as recorded on video tape (which can unfortunately not be published in the usual way). A typical set of these spatial patterns is reproduced in Fig. 14: In Fig. 14(a), two O waves are formed simultaneously near the center and at the lower right part which shortly afterwards affect a large part of the surface [Fig. 14(b)]. Somewhat later, [Fig. 14(c)] another wave forms near the left-hand side which cannot propagate very far because it can only react with sites being present in the $\text{CO-}1 \times 1$ state, but it disappears soon and a surface predominantly covered by CO is reestablished [Fig. 14(d)].

The experimental phase shifts between periodic perturbation and the response of the system had been reproduced in Figs. 7(a) and 7(b). Again the computer simulations yield a qualitatively similar result as can be seen from Fig. 7(c). The latter data were obtained with the use of an increased CO desorption probability (60%, corresponding to about 10 K temperature modulation), since otherwise the statistical fluctuations were too large.

IV. DISCUSSION

Autonomous oscillations in the catalytic CO oxidation at a Pt(100) surface are usually rather irregular and their shapes were never quite reproducible. (This contrasts with

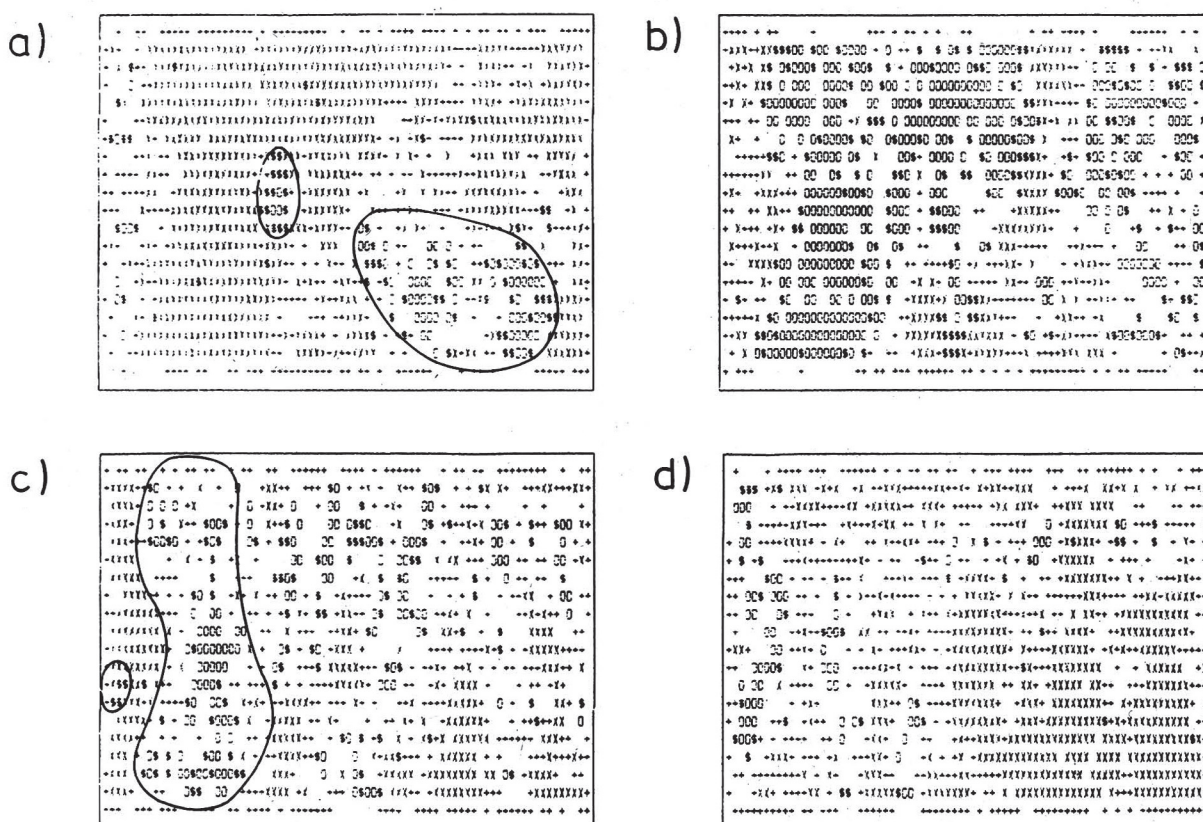


FIG. 14. Computer simulations of the spatial distributions at various times of the modulated oscillations. $\times = \text{CO-}1 \times 1$; $+$ = CO-hex; blank = empty hex; $\$$ = empty 1×1 ; $o = \text{O-}1 \times 1$. The large encircled area in (c), which is essentially covered by hex and $\text{O-}1 \times 1$, blocks an oxygen wave starting on the adjacent empty 1×1 sites at the left edge.

the recently investigated Pt(110) surface.¹⁹) Occasionally, periodic oscillations occur which are, however, usually only stable over a limited number of periods.⁶ Spatially resolved experiments by using the scanning LEED technique demonstrated that these regular oscillations resulted from waves of surface phase transformation emanating repeatedly near the same edge of the sample and propagating across the whole surface area.⁸ Such a wave might most probably start from that location which had most time to recover (i.e., from where the previous one had started), but due to statistical fluctuations the onset of the reaction may also be triggered at other patches and in different time intervals. This then leads to aperiodic behavior.

Quite similar effects were observed with the computer simulations of the autonomous oscillations if the surface was assumed to be uniform.⁹ Only with certain sets of input parameters (determining the relative speed of propagation of the reaction front, reestablishment of CO coverage and CO desorption probability) did such a uniform system undergo self-organization into large-amplitude regular oscillations for which again an oxygen wave started in periodic intervals near the same location of the lattice.

This situation changes quite pronouncedly if the system is subject to a periodic modulation of oxygen pressure or temperature. Now the oscillations are much more regular, although the phase shift and particularly the amplitude still did not become perfectly constant. The scanning LEED experiments showed that the reactive removal of adsorbed CO started near the O₂ pressure maximum and affected the whole surface area within 10 s. The wave-like propagation of this effect is no longer very pronounced, and after this short interval the whole surface apparently varies its state quite in phase. This is certainly caused by the fact that now the whole area is strongly coupled to the periodic variation of the control parameter, while in the absence of this perturbation, the occurrence of regular oscillations depends on a rather fragile coupling across the surface area.

The computer simulations agree quite well with this picture. In the case of harmonic entrainment with large forcing amplitude wave propagation was largely suppressed, but the reactive removal of CO started at about the same time (maximum of desorption probability) at various places. This gave rise to only local inhomogeneities, while the system as a whole stayed essentially in phase.

Obviously, the fluctuations inherent to the autonomous oscillations of the present system (either due to limited stability of the experimental setup or due to the stochastic nature of the elementary steps) are responsible for their usually irregular shapes. Periodic external perturbations are, however, able to cause a more regular behavior by affecting the whole surface area simultaneously.

The phenomenon of entrainment (i.e., synchronization) of an autonomously oscillating system by an external periodic perturbation has already been studied in detail with homogeneous chemical reactions as well as with appropriate mathematical models.¹⁰⁻¹³ Usually entrainment, associated with phase-locking, occurs over a finite range of the forcing frequency ν_{mod} which is called an entrainment band, and ν_{mod} is related with the main frequency of the response ν_r

through

$$\frac{l}{k} \nu_{\text{mod}} \approx \nu_r,$$

where l and k are integers, and the ratio l/k is called the order of entrainment.

The experimental results summarized in Fig. 5 show harmonic entrainment and its breakdown towards high ν_{mod} . In the computer simulations, there is evidence for harmonic as well as $\frac{1}{2}$ subharmonic entrainment in accordance with the mentioned concepts. A full exploration would require the determination of the so-called phase diagram in which the behavior of the system is studied under the influence of varying perturbation frequency *as well as amplitude*. Such a phase diagram was for example evaluated theoretically for the periodically forced Brusselator model²⁰ and exhibits regions of harmonic, subharmonic, and superharmonic entrainment as well as quasiperiodic domains and chaotic response. Systematic experimental investigation of these effects appears more feasible in future work with the Pt(110) surface which exhibits much more regular behavior of the autonomous oscillations than the Pt(100) surface used in the present study, which was of more exploratory character. In any case the results demonstrate clearly the transferability of the concepts for forced nonlinear oscillations.

V. SUMMARY

Periodic modulation of a control parameter (oxygen partial pressure or temperature) causes forced oscillations in the catalytic CO oxidation over Pt(100) as probed by work function ($\Delta\phi$) and LEED measurements. The experimentally observed features could be qualitatively well reproduced by computer simulations.

Autonomous oscillations are usually rather irregular and are synchronized across the probed surface area by propagating waves of structural transformation. By contrast, periodic modulation of adsorption/desorption rates via p_{O_2} or T causes the oscillations to become regular through phase-locking between perturbation and response typically within about 10 cycles. The structural transformation of the surface structure occurs now essentially in phase over the whole surface area.

The phase shift between perturbation and system response varies between 0 and π with increasing modulation frequency ν_{mod} in a similar way as a (damped) forced linear oscillator. Harmonic entrainment, however, is restricted to certain ranges of ν_{mod} . At higher ν_{mod} the system tends to period doubling (i.e., subharmonic entrainment) and finally exhibits irregular behavior. These effects are qualitatively in line with the general experience with forced nonlinear oscillations.

ACKNOWLEDGMENTS

The authors are indebted to H. Herz for technical assistance and to P. R. Norton for providing the single crystal sample. Financial support by the Stiftung Volkswagenwerk and by the Deutsche Forschungsgemeinschaft (SFB 128) is gratefully acknowledged.

- ¹G. Ertl, P. R. Norton, and J. Rüstig, *Phys. Rev. Lett.* **49**, 177 (1982).
- ²P. M. Cox, G. Ertl, R. Imbihl, and J. Rüstig, *Surf. Sci.* **134**, L517 (1983).
- ³P. R. Norton, P. E. Bindner, K. Griffiths, T. E. Jackman, and J. Rüstig, *J. Chem. Phys.* **80**, 3859 (1984).
- ⁴R. C. Yeates, J. E. Turner, A. J. Gellmann, and G. A. Somorjai, *Surf. Sci.* **149**, 175 (1985).
- ⁵M. P. Cox, G. Ertl, and R. Imbihl, *Phys. Rev. Lett.* **54**, 1725 (1985).
- ⁶M. Eiswirth, R. Schwankner, and G. Ertl, *Z. Phys. Chem.* **144**, 59 (1985).
- ⁷R. Imbihl, M. P. Cox, G. Ertl, H. Müller, and W. Brenig, *J. Chem. Phys.* **83**, 1578 (1985).
- ⁸R. Imbihl, M. P. Cox, and G. Ertl, *J. Chem. Phys.* **84**, 3519 (1986).
- ⁹P. Möller, K. Wetzl, M. Eiswirth, and G. Ertl, *J. Chem. Phys.* **86**, 5328 (1986).
- ¹⁰For a recent review, see F. W. Schneider, *Annu. Rev. Phys. Chem.* **36**, 347 (1985).
- ¹¹S. A. Pugh, M. Schell, and J. Ross, *J. Chem. Phys.* **85**, 868, 879 (1986).
- ¹²J. L. Hudson, P. Lamba, and J. C. Mankin, *J. Phys. Chem.* **90**, 3430 (1986).
- ¹³W. Geiseler and T. W. Taylor, *Ber. Bunsenges. Phys. Chem.* **89**, 641 (1985).
- ¹⁴F. Buchholtz and F. W. Schneider, *J. Am. Chem. Soc.* **105**, 7450 (1985).
- ¹⁵H. Herz, H. Conrad, and J. Küppers, *J. Phys. E* **12**, 369 (1979).
- ¹⁶C. Chatfield, *The Analysis of Time Series: Theory and Practice* (Chapman and Hall, London, 1975).
- ¹⁷A. Barrie, in *Handbook of x-ray and Ultraviolet Photoelectron Spectroscopy*, edited by D. Briggs (Heyden and Son, London, 1977), p. 84.
- ¹⁸R. J. Schwankner, Thesis, Universität München (1985).
- ¹⁹M. Eiswirth and G. Ertl, *Surf. Sci.* **177**, 90 (1986).
- ²⁰T. Kai and K. Tomita, *Progr. Theor. Phys.* **61**, 54 (1979).